Analytical Biochemistry 409 (2011) 267–272

Contents lists available at ScienceDirect

Analytical Biochemistry

journal homepage: www.elsevier.com/locate/yabio

Biacore analysis with stabilized G-protein-coupled receptors

Rebecca L. Rich [a], James Errey [b], Fiona Marshall [b], David G. Myszka [a,*]

[a] Center for Biomolecular Interaction Analysis, University of Utah School of Medicine, Salt Lake City, UT 84132, USA
[b] Heptares Therapeutics, Biopark, Welwyn Garden City, Hertfordshire AL7 3AX, UK

ARTICLE INFO

Article history:
Received 8 September 2010
Received in revised form 4 October 2010
Accepted 6 October 2010
Available online 20 October 2010

Keywords:
Surface plasmon resonance (SPR)
Protein–protein
Kinetics

ABSTRACT

Using stabilized forms of β_1 adrenergic and A_{2A} adenosine G-protein-coupled receptors, we applied Biacore to monitor receptor activity and characterize binding constants of small-molecule antagonists spanning more than 20,000-fold in affinity. We also illustrate an improved method for tethering His-tagged receptors on NTA (carboxymethylated dextran preimmobilized with nitrilotriacetic acid) chips to yield stable, high-capacity, high-activity surfaces as well as a novel approach to regenerate receptor binding sites. Based on our success with this approach, we expect that the combination of stabilized receptors with biosensor technology will become a common method for characterizing members of this receptor family.

Since 1990, Biacore biosensors have been used to study protein interactions in real time without labeling [1], and the past 5 years has seen a significant surge in the application of the technology for small-molecule analysis [2,3]. In contrast, the application of biosensors to study membrane-associated systems such as G-protein-coupled receptors (GPCRs)[1] is still in its infancy [4–9].

The challenges of studying membrane-associated receptors with optical biosensors are 2-fold. First, most GPCRs are expressed at low levels and are unstable when extracted from the cell membrane. This makes it tricky to immobilize these receptors onto the sensor surface while maintaining high levels of activity. Second, the ligands for most GPCRs have low molecular weights (e.g., histamine [111 Da], serotonin [176 Da]). This places an added burden on surface plasmon resonance (SPR) biosensor technology, which is mass based.

We envisioned that the approach of engineering stabilized GPCRs [10,11] for structural analysis [12] could provide excellent reagents for biosensor analysis. To validate this method, we used two receptors that contain point mutations that improve their thermostability and conformational homogeneity: a turkey β_1 adrenergic receptor (β_1AR*, with mutations R68S, M90V, Y227A, A282L, F237A, and F338M) [13,14] and a human A_{2A} adenosine receptor (A_{2A}R*, with mutations A54L, T88A, K122A, and V239A) [12,15].

We illustrate how Biacore technology allowed us to establish the benefits and limitations of different capturing methods and to confirm the activity and stability of the immobilized receptors. In addition, we provide examples of the high-quality kinetic and affinity data available from Biacore analysis of GPCRs. Our success in combining stabilized receptors with the biosensor technology demonstrates the potential of this approach and should encourage the development of additional reagents for these challenging receptor systems.

Materials and methods

Reagents and instrumentation

Studies were performed at 25 °C using Biacore 2000 and S51 optical biosensors equipped with NTA (carboxymethylated dextran preimmobilized with nitrilotriacetic acid) sensor chips (preconditioned with three 1-min pulses of 350 mM ethylenediaminetetraacetic acid [EDTA] in running buffer and charged for 3 min with 500 μM Ni^{2+} in running buffer) and equilibrated with running buffer (20 mM Tris–HCl [pH 7.8], 350 mM NaCl, and 0.1% *n*-dodecyl-β-D-maltopyranoside [DM] supplemented with 1 or 5% dimethyl sulfoxide [DMSO]). Compounds were purchased from Sigma and Tocris, detergent was purchased from Anatrace, sulfo-*N*-hydroxysuccinimide (sulfo-NHS) was obtained from Bio-Rad, 1-ethyl-3-(3-dimethylaminpropyl)-carbodiimide hydrochloride (EDC) was obtained from GE Healthcare, and general laboratory reagents were purchased from Sigma and Fisher Scientific.

* Corresponding author. Fax: +801 585 3015.
E-mail address: dmyszka@cores.utah.edu (D.G. Myszka).

[1] *Abbreviations used:* GPCR, G-protein-coupled receptor; SPR, surface plasmon resonance; β_1AR, β_1 adrenergic receptor; A_{2A}R, A_{2A} adenosine receptor; NTA, carboxymethylated dextran preimmobilized with nitrilotriacetic acid; EDTA, ethylenediaminetetraacetic acid; DM, *n*-dodecyl-β-D-maltopyranoside; DMSO, dimethyl sulfoxide; sulfo-NHS, sulfo-*N*-hydroxysuccinimide; EDC, 1-ethyl-3-(3-dimethylaminpropyl)-carbodiimide hydrochloride; FBS, fetal bovine serum; CHS, cholesteryl hemisuccinate tris salt; SDS–PAGE, sodium dodecyl sulfate–polyacrylamide gel electrophoresis; RU, resonance units; XAC, xanthine amine congener; DPCPX, 8-cyclopentyl-1,3-dipropylxanthine.

0003-2697/$ - see front matter © 2010 Elsevier Inc. All rights reserved.
doi:10.1016/j.ab.2010.10.008

Receptor expression, solubilization, and purification

Receptors were expressed in *Trichoplusia ni* cells using the Fast-Bac expression system (Invitrogen). *T. ni* cells were grown in suspension in flasks with Ex-Cell 405 medium supplemented with 5% fetal bovine serum (FBS) and 1% chemically defined lipids (Invitrogen). Cells were infected with recombinant virus when cultures reached a density of 6×10^6 cells/ml; virus was added at a multiplicity of infection of 1. An equal volume of fresh medium was added immediately afterward. Cells were harvested by centrifugation 72 h postinfection.

All membrane preparation and solubilization steps were carried out with ice-cold buffers with the inclusion of the protease inhibitors 4-(2-aminoethyl) benzenesulfonyl fluoride hydrochloride (0.5 mM), leupeptin (2.5 μg/ml), and pepstatin A (3.5 μg/ml). Cells were pelleted from 1.5 L of culture, homogenized, and resuspended in 70 ml of buffer B (40 mM Tris–HCl [pH 7.6], 300 mM NaCl, 5% glycerol, 0.001% cholesteryl hemisuccinate [CHS], and 10 μM ZM 241385 or alprenolol). Membranes were first pelleted by centrifugation at 235,000*g* for 1 h, and after removal of the supernatant, membranes were resuspended in 70 ml of buffer B with the addition of two tablets of Complete EDTA free protease inhibitor tablets (Roche) and subsequently were solubilized by the addition of 1.5% DM for 1 h on ice, followed by centrifugation at 235,000*g* for 60 min to remove unsolubilized material.

All protein purification steps were carried out at 4 °C. The solubilized material was applied to a 5-ml Ni–NTA superflow cartridge (Qiagen) preequilibrated with buffer B with the addition of 0.15% DM. The column was washed at 1 ml/min with 10 column volumes of the same buffer and then eluted with a linear gradient (15 column volumes) from 5 to 400 M imidazole in buffer B supplemented with 0.15% DM. Protein was detected with an online detector to monitor A_{280}, and column fractions were collected and analyzed by sodium dodecyl sulfate–polyacrylamide gel electrophoresis (SDS–PAGE) gel. Fractions containing the approximately 35-kDa protein were pooled and concentrated using a YM50 Amicon ultrafiltration membrane to a final volume of 200 μl. The protein sample was applied to a 10/30 S200 size exclusion column preequilibrated with buffer B with the addition of 0.1% DM (or exchange detergent) and eluted at 0.5 ml/min. Protein was detected with an online detector to monitor A_{280}, and column fractions were collected and analyzed by SDS–PAGE gel. Fractions containing the approximately 35-kDa protein were pooled and concentrated using a YM50 Amicon ultrafiltration membrane to a final concentration of 10 mg/ml and were stored at −80 °C.

NTA captures of β_1AR and A_{2A}R**

For direct NTA capture, the purified receptor (either β_1AR*–His10 or A_{2A}R*–His10) was diluted 30 to 300× in running buffer and injected at 5 μl/min to achieve capture levels of more than 10,000 resonance units (RU). For capture–coupling, a flow cell surface was activated for 5 min (at 10 μl/min) with 1:1 0.1 M sulfo-NHS/0.4 M EDC prior to injection of the receptor. Both the captured and captured–coupled receptor surfaces were washed with running buffer for at least 1 h. Activity of the receptor surfaces was evaluated using propranolol (for β_1AR*) and xanthine amine congener (XAC, for A_{2A}R*) injected across the surfaces at 100 μl/min.

Regeneration of captured–coupled β_1AR and A_{2A}R* surfaces*

At the end of each binding cycle, the GPCR surfaces were regenerated with a weak-affinity antagonist (2 × 2-min injection of 200 μM L-748,337 for β_1AR* and 2 × 1-min injection of 100 μM PSB 1115 for A_{2A}R*), followed by an EXTRACLEAN step and an injection of running buffer.

Kinetic characterization of β_1AR and A_{2A}R* antagonists*

High-affinity, small-molecule antagonists (249–504 Da, $K_D < 1$ μM) were each tested in triplicate in 3-fold dilution series for binding to β_1AR* or A_{2A}R* in running buffer containing 1% DMSO. All samples were injected at a flow rate of 100 μl/min, and when necessary the surfaces were regenerated with PSB 1115 or L-748,337.

Equilibrium analyses of lower affinity β_1AR antagonists*

Lower affinity β_1AR* analytes ($K_D > 1$ μM) were tested in duplicate in a 2-fold dilution series starting at 100 μM in running buffer containing 5% DMSO. All samples were injected at a flow rate of 90 μl/min, and a DMSO calibration series was used to correct for the excluded volume effect.

Data processing and analysis

All biosensor data processing and analysis was performed using Scrubber2 (BioLogic Software). All responses were double referenced [16]. For kinetic analyses, data were globally fit to a 1:1 interaction model that included a term for mass transport to obtain binding parameters. For equilibrium analyses, the responses at equilibrium were plotted against the analyte concentration and fit to a simple 1:1 binding isotherm.

Results

Capturing approaches for β_1AR and A_{2A}R**

Using β_1AR* as an example, Fig. 1 shows two approaches for tethering His-tagged GPCRs to NTA sensor surfaces. Simply injecting β_1AR*–His10 over the Ni^{2+}-charged NTA surface produced the green response shown in Fig. 1A. Although the receptor was captured to a high density (>10,000 RU), it gradually dissociated from the NTA surface. This dissociation can complicate the analyte binding responses and lead to a loss of surface activity. Unfortunately, this level of dissociation from NTA surfaces is fairly typical for His-tagged proteins.

To produce stable receptor surfaces, we employed an alternative approach that we call capture–coupling. This method is a hybrid of capture and amine coupling chemistry. In capture–coupling, the nickel-charged NTA surface is activated with an EDC/sulfo-NHS mixture (from −375 to −75 s in Fig. 1A) prior to injection of the receptor, as illustrated by the blue response in Fig. 1A. The His tag serves to preconcentrate the receptor onto the surface for subsequent covalent crosslinking via the activated carboxyl groups. This method is milder than the standard preconcentration step for amine coupling, which involves dropping the pH below the isoelectric point of the protein and placing the ligand in a low-salt buffer. Using capture–coupling, the β_1AR* receptor surface displayed significantly less postimmobilization drift (Fig. 1A, blue sensorgram).

To establish that capture–coupling did not compromise the receptor's activity, propranolol (259 Da) was injected across the directly NTA-captured and capture–coupled β_1AR* surfaces (Fig. 1B). The antagonist bound to both surfaces, demonstrating in each case that the receptor was active. The responses fit well to a 1:1 interaction model that yielded similar binding constants ($k_a = 9.40\ (6) \times 10^5\ M^{-1}\ s^{-1}$, $k_d = 7.80\ (4) \times 10^{-3}\ s^{-1}$, and $K_D = 8.3\ (7)$ nM for the captured surface and $k_a = 1.57\ (4) \times 10^6\ M^{-1}\ s^{-1}$, $k_d = 8.50\ (2) \times 10^{-3}\ s^{-1}$, and $K_D = 5.4\ (2)$ nM for the captured–coupled surface, where numbers in parentheses are standard errors),

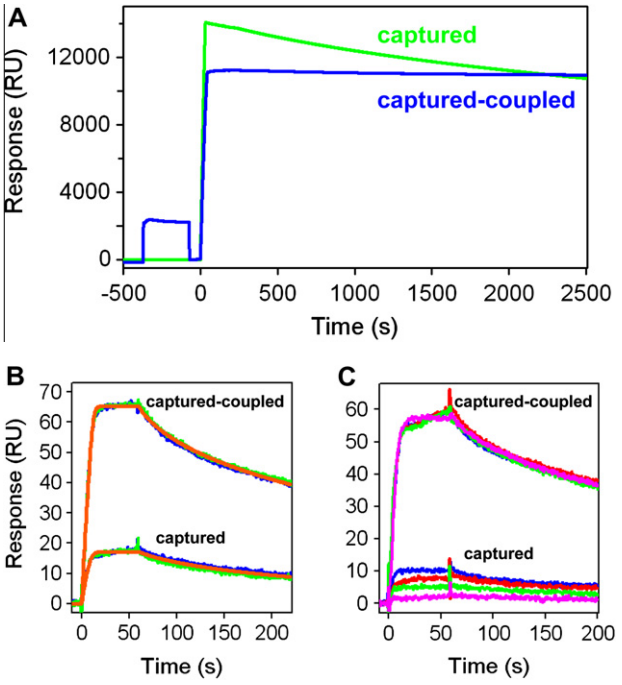

Fig.1. NTA capture methods of His-tagged GPCRs. (A) Sensorgrams for direct capture (green) and capture–couple (blue) of His-tagged β_1AR*. (B) Blue and green traces represent duplicate responses for 500 nM propranolol binding to directly captured and captured–coupled β_1AR*. The first propranolol injection over both surfaces is shown in blue, and the second is shown in green. The orange lines depict the fit of a 1:1 interaction model to each data set. (C) Replicate responses for 500 nM propranolol tested over 28 h (sample order was blue, red, green, and then pink) for binding to the captured–coupled and captured β_1AR* surfaces. (For interpretation of the references to color in this figure legend, the reader is referred to the Web version of this article.).

indicating that capture–coupling did not alter the receptor's binding activity.

When comparing the response levels achieved for propranolol from the two coupling methods, it is clear that the captured–coupled surface produced a significantly higher binding response than the directly captured surface (in this example, the response is more than three times larger for the captured–coupled surface) (Fig. 1B). The lower response for the captured receptor surface likely stems from the decay of the receptor from the NTA ligand. Importantly, the R_{max} determined for the captured–coupled β_1AR* surface suggests that the immobilized receptor was approximately 75% active.

The differences in stability and activity of the two β_1AR* surfaces are even more apparent in Fig. 1C. Four replicate injections of propranolol (tested at 7-h intervals) across the captured–coupled receptor surface overlay, confirming that this surface was stable over more than 24 h. In contrast, over the same time period, the NTA-captured-only receptor surface lost all activity. Together, the data in Fig. 1 demonstrate that capture–coupling produces high-density, active, and stable surfaces for this His-tagged receptor. Similar results were obtained for His-tagged A_{2A}R* (data not shown). Based on the success of this method, capture–coupling was used to generate the data reported throughout the rest of the study.

Regeneration of GPCR surfaces

One of the limitations introduced by capture–coupling is that the receptor is now covalently immobilized to the surface. This eliminates the possibility of stripping the receptor from the surface and recapturing it as a means of regenerating tightly bound compounds. Therefore, we are left with two options for regeneration: (i) washing the receptor surfaces with buffer until the bound analyte dissociates (often requiring >1-h wash phases) or (ii) using a regeneration method that removes bound analyte without affecting receptor activity. Unfortunately, we find that regeneration conditions commonly used for protein/protein interactions (e.g., dilute phosphoric acid, base, high salt) are often ineffective at regenerating small-molecule binding sites [17], and harsher conditions would likely be detrimental to the GPCR surfaces. Therefore, to regenerate the β_1AR* and A_{2A}R* systems, we developed an alternative approach that we refer to as *displacement regeneration.*

In displacement regeneration, bound analytes are displaced by a weak-affinity compound injected at high concentrations. This regeneration method works by saturating the available receptor binding sites, thereby blocking rebinding of the high-affinity analyte. Because this method involves passive displacement, it is most appropriate for analytes that are limited by mass transport, which we found is the case for many of the β_1AR and A_{2A}R antagonists.

Fig. 2 shows an example of the regeneration tests of A_{2A}R*. In this work, the analyte of interest, ZM-241,385, was injected for 1 min and its dissociation from the surface was monitored for 2 min. (Note that ZM-241,385 shows an apparent slow dissociation rate). To displace the bound ZM-241,385, a weak A_{2A}R antagonist, PSB 1115 ($K_D \sim 1$ μM), was injected twice at a concentration of 100 μM during the dissociation phase. No binding response is visible for PSB 1115 in the main figure because these data were double referenced. In double referencing, buffer was injected instead of ZM-241,385, but PSB 1115 was still injected during regeneration. Once the data are fully processed, this double referencing step essentially removes the binding response for PSB 1115 because it occurs in every cycle. To demonstrate that in fact PSB 1115 is binding during the regeneration steps, the inset in Fig. 2 shows the raw data for one of the binding cycles; here the responses for PSB 1115 up to approximately 50 RU are apparent.

By the end of the second PSB 1115 injection, all ZM-241,385 appears to be displaced from the receptor surface (Fig. 2, main panel). The ZM-241,385 binding and PBS 1115 regeneration cycles were repeated three times to demonstrate that this regeneration condition is sufficient to remove bound ZM-241,385 from A_{2A}R* without reducing receptor activity (note the excellent overlay of the black, green, and blue sensorgrams in the main panel of Fig. 2). A similar regeneration approach was successfully developed for β_1AR* using 200 μM L-748,337 as the displacement analyte (data not shown).

Kinetic analyses of β_1AR and A_{2A}R* antagonists*

Having optimized immobilization and regeneration conditions for β_1AR* and A_{2A}R*, we next applied the Biacore assay to

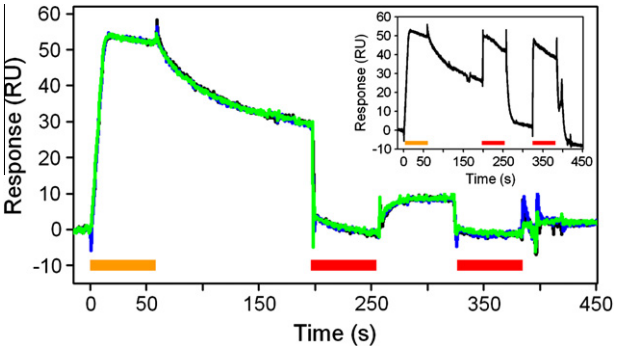

Fig.2. Regeneration of captured–coupled GPCR surfaces. The main panel shows an overlay of three binding cycles for A_{2A}R*: injection of 300 nM ZM-241,385 (highlighted by the orange bar), followed by buffer wash for 2 min and two 1-min injections of 100 μM PSB 1115 (highlighted by the red bars). The inset shows raw responses for these binding cycles. (For interpretation of the references to color in this figure legend, the reader is referred to the Web version of this article.).

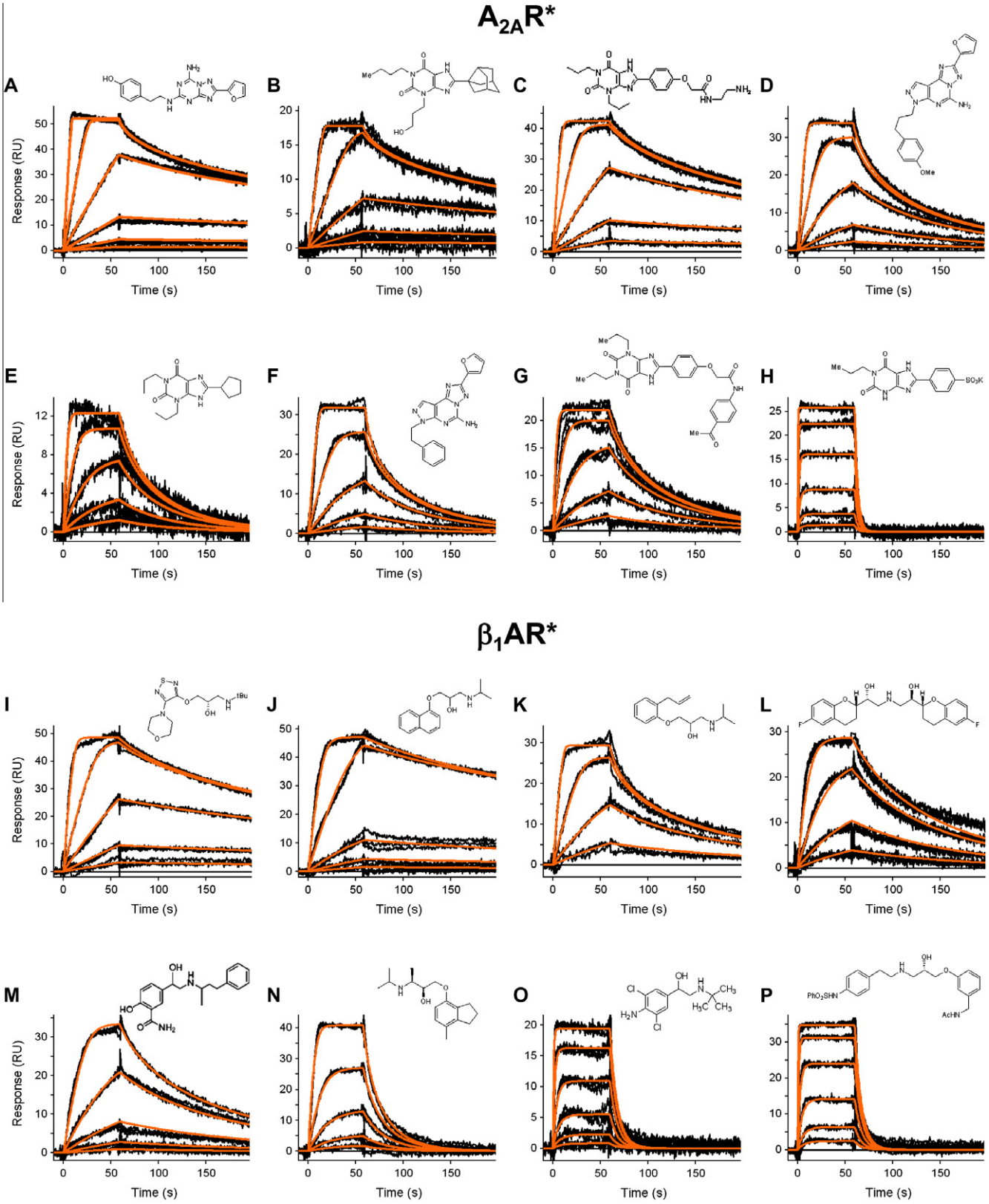

Fig.3. Kinetic analyses of $A_{2A}R^*$ and β_1AR^* antagonists. Each compound was tested in triplicate in a 3-fold dilution series, and the responses were fit to a 1:1 interaction model. Antagonist structures are shown in the insets; compound identities and binding parameters determined from the fits are listed in Table 1.

characterize the binding kinetics of eight antagonists (which ranged in size from 249 to 504 Da) to each receptor. Fig. 3 presents the response data for a concentration series of each compound. Triplicate injections of each concentration overlay very well, demonstrating that the observed binding responses were reproducible. In addition, each data set could be globally fit to a 1:1 interaction model. A summary of the binding constants is provided in Table 1.

Table 1
Binding constants for GPCR/compound interactions determined at 25 °C

Panel[a]	$A_{2A}R^*$ analyte	MW (Da)	k_a (M^{-1} s^{-1})	k_d (s^{-1})	K_D (nM)
3A	ZM-241,385	337	$1.33\ (6) \times 10^7$	$3.80\ (2) \times 10^{-2}$	2.8 (2)
3B	PSB 36	386	$5.10\ (6) \times 10^6$	$3.60\ (4) \times 10^{-2}$	7 (1)
3C	XAC	428	$1.39\ (2) \times 10^6$	$1.12\ (1) \times 10^{-2}$	8.1 (1)
3D	SCH 442416	389	$2.60\ (8) \times 10^6$	$5.30\ (2) \times 10^{-2}$	20.2 (9)
3E	DPCPX	304	$1.20\ (5) \times 10^7$	$6.00\ (3) \times 10^{-1}$	50 (30)
3F	SCH 58261	345	$1.00\ (3) \times 10^6$	$6.60\ (2) \times 10^{-2}$	66 (1)
3G	MRS 1706	504	$3.36\ (7) \times 10^5$	$3.47\ (8) \times 10^{-2}$	103 (3)
3H	PSB 1115	388	$3.90\ (1) \times 10^5$	$3.18\ (9) \times 10^{-1}$	810 (30)
	β_1AR^* analyte				
3I	Timolol	316	$9.40\ (1) \times 10^5$	$6.94\ (8) \times 10^{-3}$	7.4 (1)
3J	Propranolol	259	$4.50\ (1) \times 10^5$	$3.28\ (4) \times 10^{-3}$	7.2 (2)
3K	Alprenolol	249	$1.31\ (4) \times 10^6$	$2.49\ (7) \times 10^{-2}$	19.0 (1)
3L	Nebivolol	405	$2.76\ (5) \times 10^5$	$1.50\ (3) \times 10^{-2}$	31.8 (1)
3M	Labetalol	328	$2.64\ (6) \times 10^5$	$2.51\ (5) \times 10^{-2}$	95 (3)
3N	ICI 118,551	277	$2.40\ (7) \times 10^5$	$8.50\ (3) \times 10^{-2}$	350 (10)
3O	Clenbuterol	277	$2.47\ (9) \times 10^5$	$1.33\ (5) \times 10^{-1}$	540 (30)
3P	L-748,337	498	$2.37\ (6) \times 10^5$	$1.41\ (4) \times 10^{-1}$	600 (20)
4A	Butoxamine	267	–	–	5150 (20)
4B	Serotonin	176	–	–	14,170 (50)
4C	Atenolol	266	–	–	49,200 (200)
4D	Methylergonovine	339	–	–	49,600 (300)
4E	Ergonovine	325	–	–	84,100 (800)

Note. Numbers in parentheses are standard errors. –, not determined (K_D obtained from equilibrium analysis).
[a] Key to data sets shown in Figs. 3 and 4.

Equilibrium analyses of lower affinity interactions

A powerful feature of Biacore technology is the ability to detect and quantitate relatively weak interactions ($K_D > 1$ μM). To explore this possibility with the GPCR systems, we characterized the binding of five lower- affinity compounds against β_1AR^*. As shown in Fig. 4, each of these compounds bound in a concentration-dependent manner, and the responses were reproducible. Because they all have very fast dissociation rates, they reached equilibrium rapidly during the association phase. The responses at equilibrium all fit well to a simple 1:1 binding model, as shown in Fig. 4F. The affinities for these compounds ranged from approximately 5 to 85 μM (Table 1).

Discussion

We showed previously how Biacore could be used to study native GPCRs from both purified and crude preparations [4–9]. We developed assays to identify solubilization and purification conditions [4–6], and we applied the technology to characterize the binding kinetics of antibodies, natural ligands, and small molecules ranging in affinity from picomolar (pM) to millimolar (mM) [7–9].

In this article, we illustrated the advantages of using stabilized forms of GPCRs as ligands in Biacore experiments. Because a key requirement for the biosensor technology is that the ligand be active, a major advantage of the stabilized receptors is that they can be prepared with high overall activity and conformational homogeneity. (The β_1AR^* and $A_{2A}R^*$ that we used in this study were engineered to be in an antagonist conformation [10,12–15].) This high binding activity allows us to achieve relatively large binding responses even for small analytes. The conformational homogeneity likely contributes to the fact that the binding response data for all of the compounds studied were reproducible and could be fit to a simple model.

However, even with active and stable starting material, we needed to optimize the receptor immobilization conditions by employing a capture–coupling approach. This method worked well with both the His-tagged β_1AR^* and $A_{2a}R^*$ receptor systems, providing high-capacity surfaces that were stable over time. However, we should stress that with any new receptor system, it is important to run control experiments to ensure that the capture–coupling approach does not significantly affect receptor binding activity.

We developed a novel regeneration method that uses high concentrations of a weak binding analyte to passively dissociate a

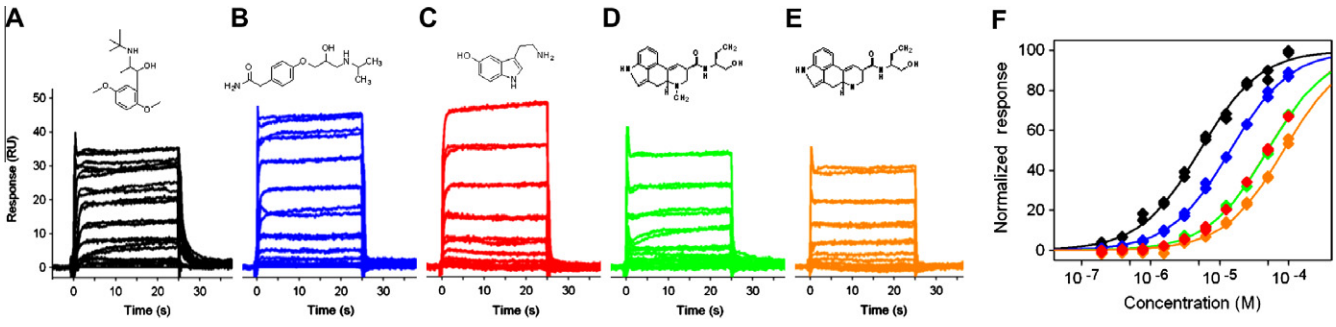

Fig.4. Equilibrium analyses of five lower- affinity β_1AR analytes. Each compound was tested in duplicate in a 2-fold dilution series starting at 100 μM. Responses at equilibrium (t = 10–20 s) were plotted against compound concentration and fit to a simple binding isotherm. Analyte structures are shown in the insets; compound identities and affinities from the isotherms are listed in Table 1.

bound compound. This method will be most effective at regenerating analytes with fast association rates. These systems tend to be mass transport limited and can be easily displaced from the sensor surface by blocking rebinding as compared with a compound that has an inherently slow dissociation rate. Given the simplicity of this approach, we would encourage biosensor users to try displacement regeneration when they encounter slowly dissociating analytes with their own systems.

Using optimized immobilization and regeneration methods, we were able to characterize the binding of a range of small-molecule analytes to both β_1AR* and A_{2a}R*. This series of compounds displayed a wide range of association and dissociation rate constants that produced a nearly 300-fold span in affinity. Having established the conditions for analysis of the stabilized receptors, we are in the process of transferring the methodology to study native forms of these same receptors. Biacore should provide an excellent method of assessing in detail whether and how the stabilizing mutations change the recognition properties of the receptors.

Finally, we demonstrated that it is possible to characterize the affinity of relatively weak compounds ($K_D \sim 10$–100 μM) binding to these receptors. These results hint at the potential of using Biacore to screen fragment libraries against GPCRs. One of our concerns, however, is that high concentrations of compounds used in fragment screening (100–500 μM) may show high levels of nonspecific binding to the receptor surfaces. We are currently investigating whether this will be the case. But an additional advantage of using stabilized receptors is that they can be crystallized [12] to confirm hits from a fragment library and identify binding modes for these compounds, which would be a useful in elaborating the hits.

Of course, engineering stabilized receptors requires a substantial amount of effort. But it is encouraging to see that these types of reagents are excellent tools for biosensor analysis. We are certain that the combination of stabilized receptors and biosensor technology will provide new insights into receptor structure/function and that the high quality of direct binding data will have a positive impact on drug discovery.

Acknowledgment

This work was funded by a Grant (GM 071697) awarded to D.G.M. by the National Institutes of Health.

References

[1] (a) S. Löfås, B. Johnsson, A novel hydrogel matrix on gold surfaces in surface plasmon resonance sensors for fast and efficient covalent immobilization of ligands, J. Chem. Soc. Chem. Commun. (1990) 1526–1528;
(b) S. Löfås, M. Malmqvist, I. Rönnberg, E. Stenberg, B. Liedberg, I. Lundström, Bioanalysis with surface plasmon resonance, Sens. Actuat. B 5 (1991) 79–84;
(c) R. Karlsson, A. Michaelsson, L. Mattsson, Kinetic analysis of monoclonal antibody–antigen interactions with a new biosensor based analytical system, J. Immunol. Methods 145 (1991) 229–240.
[2] R.L. Rich, D.G. Myszka, Survey of the year 2007 commercial optical biosensor literature, J. Mol. Recognit. 21 (2008) 355–400.
[3] R.L. Rich, D.G. Myszka, Grading the commercial optical biosensor literature: "The mighty binders,"—Class of 2008, J. Mol. Recognit. 23 (2010) 1–64.
[4] I. Navratilova, J. Sodroski, D.G. Myszka, Solubilization, stabilization, and purification of chemokine receptors using Biacore technology, Anal. Biochem. 339 (2005) 271–281.
[5] R.L. Rich, A.R. Miles, B.K. Gale, D.G. Myszka, Detergent screening of a GPCR using serial and array biosensor technologies, Anal. Biochem. 386 (2009) 98–104.
[6] I. Navratilova, M. Pancera, R.T. Wyatt, D.G. Myszka, A biosensor-based approach toward purification and crystallization of G protein-coupled receptors, Anal. Biochem. 353 (2006) 273–278.
[7] I. Navratilova, M. Dioszegi, D.G. Myszka, Analyzing ligand and small molecule binding activity of solubilized GPCRs using biosensor technology, Anal. Biochem. 355 (2006) 132–139.
[8] I. Navratilova, D.G. Myszka, R.L. Rich, Probing membrane protein interactions with real-time biosensor technology, in: E. Pebay-Peroula (Ed.), Biophysical Analysis of Membrane Proteins, Wiley–VCH, Weinheim, Germany, 2008, pp. 121–140.
[9] M. Congreve, R.L. Rich, D.G. Myszka, G. Siegal, F. Marshall, Fragment screening of stabilized G-protein coupled receptors using biophysical methods, Methods Enzymol., in press.
[10] T. Warne, M.J. Serrano-Vega, C.G. Tate, G.F. Schertler, Development and crystallization of a minimal thermostabilised G protein-coupled receptor, Protein Expr. Purif. 65 (2009) 204–213.
[11] Y. Shibata, J.F. White, M.J. Serrano-Vega, F. Magnani, A.L. Aloia, R. Grishammer, C.G. Tate, Thermostabilization of the neurotensin receptor NTS1, J. Mol. Biol. 390 (2009) 262–277.
[12] T. Warne, M.J. Serrano-Vega, J.G. Baker, R. Moukhametzianov, P.C. Edwards, R. Henderson, A.G. Leslie, C.G. Tate, G.F. Schertler, Structure of a β_1-adrenergic G-protein-coupled receptor, Nature 454 (2008) 486–491.
[13] M.J. Serrano-Vega, F. Magnani, Y. Shibata, C.G. Tate, Conformational thermostabilization of the β_1-adrenergic receptor in a detergent-resistant form, Proc. Natl. Acad. Sci. USA 105 (2008) 877–882.
[14] M.J. Serrano-Vega, C.G. Tate, Transferability of thermostabilizing mutations between β-adrenergic receptors, Mol. Membr. Biol. 26 (2009) 385–396.
[15] F. Magnani, Y. Shibata, M.J. Serrano-Vega, C.G. Tate, Co-evolving stability and conformational homogeneity of the human adenosine A_{2A} receptor, Proc. Natl. Acad. Sci. USA 105 (2008) 10744–10749.
[16] D.G. Myszka, Improving biosensor analysis, J. Mol. Recognit. 12 (1999) 279–284.
[17] G.A. Papalia, A.M. Giannetti, N. Arora, D.G. Myszka, Thermodynamic characterization of pyrazole and azaindole derivatives binding to p38 MAP kinase using Biacore T100 technology and van't Hoff analysis, Anal. Biochem. 383 (2008) 255–264.